electronic reprint

Acta Crystallographica Section B
Structural Science
ISSN 0108-7681

The incommensurate structure of $K_3In(PO_4)_2$

Alla Arakcheeva, Gervais Chapuis, Vaclav Petříček, Michal Dušek and Andreas Schönleber

Acta Crystallographica Section B
Structural Science
ISSN 0108-7681

The incommensurate structure of $K_3In(PO_4)_2$

Alla Arakcheeva,[a,b] Gervais Chapuis,[a]* Vaclav Petříček,[a,c] Michal Dušek[a,c] and Andreas Schönleber[a]

[a]Université de Lausanne, Institut de Cristallographie, BSP Dorigny, CH-1015 Lausanne, Switzerland, [b]Baikov Institute of Metallurgy, RAS, 119991 Moscow, Russia, and [c]Institute of Physics, Academy of Science of the Czech Republic, Na Slovance 2, 182 21 Praha, Czech Republic

Correspondence e-mail: gervais.chapuis@ic.unil.ch

Received 31 August 2002
Accepted 19 November 2002

The incommensurately modulated structure of $K_3In(PO_4)_2$ has been solved and refined. The origin of the modulation relates to the ordering of K cations within the hexagonal close packing of the PO_4 anions. The driving forces for the modulation of the other cations are In—P and K—P interactions. The modulation of O atoms of rigid PO_4 units follows the cations in order to stabilize the InO_6 octahedron. It is shown that the previously published three-dimensional structure refined from powder diffraction data obtained at room temperature is an average structure. Therefore the incommensurately modulated phase of $K_3In(PO_4)_2$ is the only one that has been unequivocally identified at room temperature. The origin of the modulation is discussed in comparison with the structures of Na_3InP_2, α- and β-$Na_3In(PO_4)_2$, $Na_3Fe(PO_4)_2$ and $Rb_3In(PO_4)_2$.

1. Introduction

Potassium indium double phosphate, $K_3In(PO_4)_2$, was first obtained (Zhizhin *et al.*, 2002) as powder and single-crystal specimens by sintering In_2O_3, KH_2PO_4 and K_2CO_3 at the temperatures 1173 K and 1473 K, respectively. Preliminary X-ray investigation (Zhizhin *et al.*, 2002) gave identical monoclinic unit cells for both powder and single-crystal specimens. In addition, a few weak satellite reflections, which were detected from single-crystal diffraction with a CAD-4 (Mo $K\alpha$ radiation) diffractometer, revealed the modulated character of the crystal. A powder sample of $K_3In(PO_4)_2$ was used for the crystal structure investigation with a Stadi-P (Stoe) diffractometer (Cu $K\alpha_1$; $8 < 2\theta < 100^\circ$; room temperature). The crystal structure was determined and refined by the Rietveld method (Zhizhin *et al.*, 2002) in a three-dimensional space group [$C2/c$, $a = 15.6411$ (1), $b = 11.1909$ (1), $c = 9.6981$ (1) Å, $\beta = 90.119$ (1)°; $V = 1697.53$ (3) Å^3; $Z = 8$; $\chi^2 = 4.88$, $R_p = 4.02\%$, $R_{wp} = 5.25\%$]. The profile parameters were satisfactorily refined without considering any satellite reflection. A preliminary test from single-crystal diffraction (Oxford Diffraction/CCD diffractometer, Mo $K\alpha$ radiation) showed a series of strong satellites in the ($hk0$), ($hk1$) and ($hk2$) planes. These results were in reasonable accordance with the unit-cell parameters obtained from powder refinement. The purpose of this paper is to present the results of the structural analysis of the modulated structure and explain the relationship between the modulated structure and the solution deduced from powder diffraction. The structure is also compared with other double phosphates $A_3R(PO_4)_2$, where A = K, Na and Rb and R = In, Fe, and with the Na_3InP_2 alloy. These structures can be understood as hexagonal close packings of P atoms with different distributions of R and A atoms inside the P_6 octahedra and P_5 bipyramids. This characteristic

will be used to explain the origin of the modulations in $K_3In(PO_4)_2$.

2. Experimental

2.1. Synthesis

Single crystals of $K_3In(PO_4)_2$ were prepared by sintering a stoichiometric ratio of In_2O_3, KH_2PO_4 and K_2CO_3 at 1473 K for 4 h in air. Detailed information on the preparation is given by Zhizhin *et al.* (2002).

2.2. Data collection

The data collection was performed with an Oxford Diffraction CCD diffractometer in half of reciprocal space. A standard peak search on the recorded frames resulted in 12370 peak positions. A first refinement, based on these peaks, of the unit-cell parameters and a reciprocal space reconstruction were performed with the *CrysAlis* software (Oxford Diffraction Ltd, 2001). With this procedure the ratio of the indexed peaks to the extracted peaks was rather poor. The reconstruction of the reciprocal space showed that the non-indexed reflections could be interpreted as first- and second-order satellites with the modulation vector $\mathbf{q} = \alpha\,\mathbf{a}^* + \beta\,\mathbf{b}^* + \gamma\,\mathbf{c}^*$, where α and β are approximately 0.2 and $\gamma = 0$. The coefficients α, β and γ, along with the parameters of the orientation matrix, were refined with the program *NADA* (Schönleber *et al.*, 2001); the refinement was based on the 12370 peak positions found with the standard search routine. With the unit cell and the modulation vector, more than 96% of the peaks were successfully indexed. Data integration of the recorded frames and Lorentz and polarization corrections were performed with the *CrysAlis* software (Oxford Diffraction Ltd, 2001). The systematic absences *hklm*, $h + l + m = 2n$, imply the non-primitive cell-centring vector $(1/2, 0, 1/2, 1/2)$, which corresponds to a *B* centring of the 3d unit cell. The additional reflection conditions (*hk*0*m*: $k + m = 2n$) imply two possible superspace groups: $X2/b(\alpha\beta0)0s$ and $Xb(\alpha\beta0)s$. The centrosymmetric superspace group was chosen because of the absence of a signal in the second-harmonic generation test (Zhizhin *et al.*, 2002). This choice was confirmed by the successful solution and refinement of the structure. The basic experimental data are listed in Table 1.[1]

Table 1
Experimental details.

Chemical formula	$InK_3O_8P_2$
Chemical formula weight	422.1
Cell setting, superspace group	Monoclinic, $X2/b(\alpha\beta0)0s$ with non-primitive translation X = [0.5 0 0.5 0.5]
a, b, c (Å)	15.6537 (5), 9.7357 (4), 11.1975 (4)
γ (°)	90.124 (5)
V (Å^3)	1706.49 (11)
Z	8
D_x (Mg m^{-3})	3.284 (1)
Modulation wave vector	$\mathbf{q}$ = 0.18813 (5)$\mathbf{a}^*$ + 0.21423 (3)$\mathbf{b}^*$
Radiation type	Mo $K\alpha$
No. of reflections for cell parameters	12370
θ range (°)	3–51.8
μ (mm^{-1})	4.62
Temperature (K)	293
Crystal form, colour	Cube, red
Crystal size (mm)	0.2 × 0.19 × 0.18
Diffractometer	KM4
Data collection method	CCD detector KM4CCD/ SAPPHIRE
Absorption correction	None
No. of measured, independent and observed reflections	125808, 41649, 11828
No. of main, first-order satellite and second-order satellite reflections	3328, 5420, 3080
Criterion for observed reflections	$I > 3\sigma(I)$
R_{int}	0.1
θ_{max}	51.8
Range of h, k, l, m	$-34 \Rightarrow h \Rightarrow 34$ $0 \Rightarrow k \Rightarrow 21$ $0 \Rightarrow l \Rightarrow 24$ $-2 \Rightarrow m \Rightarrow 2$
Refinement on	F
$R[F^2 > 3\sigma(F^2)], wR[F^2 > 3\sigma(F^2)], S$	0.059, 0.059, 2.03
R, wR (main reflection)	0.042, 0.042
R, wR (satellites of order 1)	0.058, 0.058
R, wR (satellites of order 2)	0.105, 0.117
No. of reflections and parameters used in refinement	11828, 364
Weighting scheme	$w = 1/[\sigma^2(F) + 0.0001F^2]$
$(\Delta/\sigma)_{max}$	0.001
$\Delta\rho_{max}$, $\Delta\rho_{min}$ (e Å^{-3})	4.16, −3.31

† Computer programs: *CrysAlis* (Oxford Diffraction Ltd, 2001); *JANA*2000 (Petříček & Dušek, 2000).

3. Structure determination

3.1. Determination and refinement of the average structure

The average structure was solved by the heavy-atom method. Atomic coordinates and equivalent isotropic displacement parameters for the average structure of $K_3In(PO_4)_2$ are compared in Table 2 with those obtained previously by Zhizhin *et al.* (2002). The splitting of the K4 atomic position (the distance K4*a*—K4*b* ∼ 1.5 Å) was well identified. The refinement converged to R = 11.8% with very large displacement ellipsoids for K and especially for O atoms. The lowest value of the R factor could only be reached for the average structure with split O positions.

The average structure is practically the same as the model described by Zhizhin *et al.* (2002). The framework is built up from vertex- and edge-sharing InO_6 octahedra and PO_4 tetrahedra. K cations surrounded by seven or eight O atoms are located in channels of the framework. This standard description is based on polyhedra of the first coordination sphere of cations. In spite of the large temperature parameters there are no obvious discrepancies with the first-coordination-sphere geometry of the average structure: the interatomic distances within the PO_4 tetrahedra and InO_6 octahedron [In—O, 2.02–2.33, ⟨2.14⟩; P—O, 1.51–1.54, ⟨1.53⟩; K—O, 2.54–

[1] Supplementary data for this paper are available from the IUCr electronic archives (Reference: SN0028). Services for accessing these data are described at the back of the journal.

Table 2
Atomic parameters of the average structure of $K_3In(PO_4)_2$.

Entries in italics indicate the corresponding data obtained by Zhizhin *et al.* (2002) for the $K_3In(PO_4)_2$ three-dimensional structure with X-ray powder diffraction data.

Atom	*x*	*y*	*z*	B_{iso}
In	−0.12399 (5)	−0.07424 (8)	0.36090 (7)	2.50 (2)
	−0.1251 (1)	*−0.0747 (1)*	*0.3623 (1)*	*3.0 (1)*
K1	0	−0.25	0.6135 (4)	3.8 (1)
			0.6146 (3)	*5.7 (1)*
K2	0	−0.25	0.1235 (4)	7.1 (2)
			0.1245 (4)	*5.1 (1)*
K3	0.2522 (2)	−0.2075 (4)	0.1202 (3)	4.50 (8)
	0.2532 (1)	*−0.2085 (2)*	*0.1276 (2)*	*3.1 (1)*
K4*a*, *p* = 0.59 (1)	0.5832 (3)	0.0979 (5)	0.6139 (3)	3.9 (1)
p = 0.58 (3)	*0.5918 (3)*	*0.0966 (4)*	*0.6085 (3)*	*3.7 (3)*
K4*b*, *p* = 0.41 (1)	−0.1749 (7)	−0.0991 (8)	0.9102 (9)	4.2 (2)
p = 0.42 (3)	*−0.1828 (3)*	*−0.1009 (6)*	*0.9015 (9)*	*3.7 (3)*
P1	0.15184 (20)	−0.0705 (3)	0.8558 (3)	2.79 (6)
	0.1498 (3)	*−0.0726 (3)*	*0.8502 (3)*	*2.1 (1)*
O11	0.1401 (5)	0.0868 (8)	0.8381 (7)	2.5 (2)
	0.1338 (3)	*0.0831 (4)*	*0.8455 (4)*	*3.2 (2)*
O12	0.1364 (8)	−0.1287 (9)	0.7289 (9)	5.2 (3)
	0.1357 (3)	*−0.1310 (5)*	*0.7270 (3)*	*3.1 (2)*
O13	0.2434 (6)	−0.1027 (15)	0.8912 (7)	4.9 (3)
	0.2448 (2)	*−0.0975 (6)*	*0.8965 (4)*	*2.8 (2)*
O14	0.0928 (6)	−0.1271 (11)	0.9489 (10)	4.3 (3)
	0.0925 (4)	*−0.1375 (5)*	*0.9421 (10)*	*2.8 (1)*
P2	0.09846 (14)	−0.0817 (3)	0.36844 (18)	1.55 (4)
	0.0999 (1)	*−0.0835 (3)*	*0.3684 (2)*	*2.6 (1)*
O21	0.1131 (7)	−0.2217 (12)	0.4344 (9)	4.3 (3)
	0.1086 (3)	*−0.2298 (5)*	*0.4192 (4)*	*3.0 (2)*
O22	0.0067 (7)	−0.0601 (17)	0.3306 (15)	8.1 (5)
	0.0086 (7)	*−0.0557 (17)*	*0.3299 (15)*	*3.2 (1)*
O23	0.1580 (11)	−0.056 (2)	0.2715 (15)	11.4 (7)
	0.1584 (11)	*−0.0724 (6)*	*0.2588 (5)*	*7.0 (2)*
O24	0.1170 (12)	0.0288 (14)	0.4535 (10)	8.4 (6)
	0.1282 (4)	*0.0202 (5)*	*0.4623 (4)*	*5.7 (2)*

3.37, ⟨2.91⟩ Å] are in a good agreement with the expected values.

Therefore, in order to understand the origin of the modulation, our description of the structure is based on the second coordination sphere of the cations (see Figs. 1*a* and 1*b*). The centres of the PO_4 tetrahedra (the P atoms) form simple hexagonal close packing of the PO_4 anions. As the second coordination sphere plays a dominant role we shall hereinafter use instead of full symbols $M(PO_4)_n$ (M = In, K; n = 4, 5, 6 for the tetrahedron, trigonal bipyramid and octahedron, respectively) a short symbol MP_n for the cationic polyhedra of the second coordination sphere.

All octahedra are occupied with K1, K2 and K3 cations ($K1P_6$, $K2P_6$ and $K3P_6$); all trigonal bipyramids are filled with In and K4 cations (InP_5 and $K4P_5$). As seen from Fig. 1(*b*), the splitting of the K4 cation is a consequence of the statistical distribution between the two tetrahedra that form the trigonal bipyramid. The ordering of K4 cations over the two P_4-tetrahedra positions is possibly the driving force for the modulations in the crystal.

3.2. Refinement of the modulated structure

The average structure derived from unsplit O atoms was used as a starting model for the refinement of the modulated structure. A first-harmonic wave for displacive modulation was refined for all cation positions except for K4. The refinement converged smoothly. The x_1–x_4 sections (Fig. 2*a*) of the Fourier synthesis, which were calculated in the vicinity of the K4*a* and K4*b* positions, revealed a step-like character of the positional modulation. The distance between the separated positions was about 1.5 Å, which fitted well with the average-structure results. Such behaviour can be modelled by a crenel function for both atoms (Petříček *et al.*, 1995). The obvious complementary character of the modulation and the condition that these positions must be fully occupied lead to the following restrictions:

$$\Delta(\mathrm{K4}b) = 1 - \Delta(\mathrm{K4}a),$$

$$x_4^0(\mathrm{K4}b) = 1/2 + x_4^0(\mathrm{K4}a) - \mathbf{q}\cdot\mathbf{r}(\mathrm{K4}a) + \mathbf{q}\cdot\mathbf{r}(\mathrm{K4}b),$$

where x_4^0 and Δ are the centre and length, respectively, of the crenel function.

The O ions are strongly bonded in the PO_4 groups and therefore it is natural to suppose that the modulation does not affect the rigidity of the PO_4 groups. $P1O_4$ was successfully refined as an entity with four harmonic waves for the translation and the rotation. The same modulation model for $P2O_4$ did not yield a satisfying result. A detailed analysis of the Fourier maps in the vicinity of this group led to the conclusion

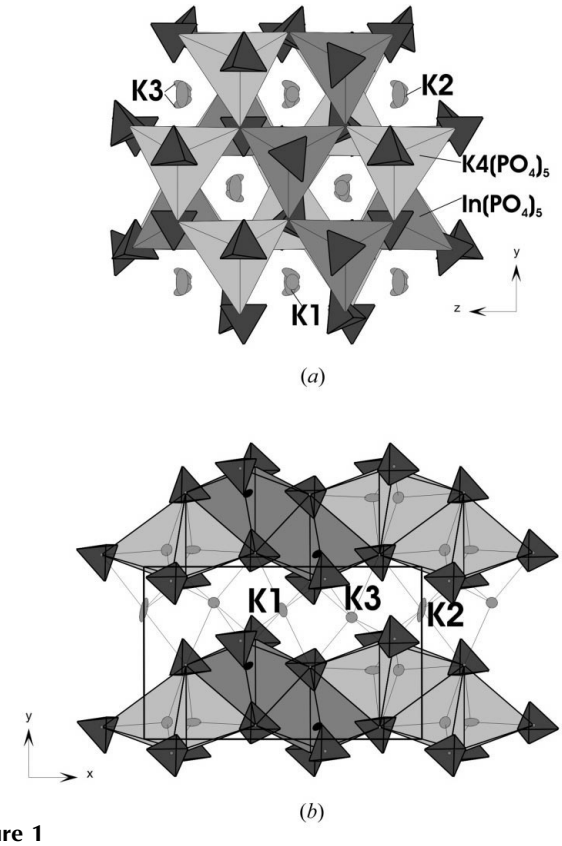

Figure 1
The average structure of $K_3In(PO_4)_2$. The $K4(PO_4)_5$ and $In(PO_4)_5$ trigonal bipyramids are shown in the (100) projection (*a*) and in the characteristic layer normal to the [001] direction (*b*); the $K1(PO_4)_6$, $K2(PO_4)_6$ and $K3(PO_4)_6$ octahedra are indicated with six K—P sticks. The split K4 cation is statistically distributed between two tetrahedra within the $K4(PO_4)_5$ bipyramid.

that three complementary crenel functions could better account for its modulation. The analogous restrictions to those used for the K4 atom are

$$\Delta(\mathrm{P2O_4}c) = 1 - \Delta(\mathrm{P2O_4}a) - \Delta(\mathrm{P2O_4}b),$$

$$x_4^0(\mathrm{P2O_4}b) = 1/2\big[\Delta(\mathrm{P2O_4}a) + \Delta(\mathrm{P2O_4}b)\big] + x_4^0(\mathrm{P2O_4}a) - \mathbf{q}\cdot\mathbf{r}(\mathrm{P2O_4}a) + \mathbf{q}\cdot\mathbf{r}(\mathrm{P2O_4}b).$$

$$x_4^0(\mathrm{P2O_4}c) = 1/2\big[\Delta(\mathrm{P2O_4}b) + \Delta(\mathrm{P2O_4}c)\big] + x_4^0(\mathrm{P2O_4}b) - \mathbf{q}\cdot\mathbf{r}(\mathrm{P2O_4}b) + \mathbf{q}\cdot\mathbf{r}(\mathrm{P2O_4}c).$$

For $P2O_4$ this model leads immediately to a satisfactory fit. The fact that several atoms are modulated discontinuously raises the question of whether the continuous functions used for all other atoms properly describe the modulation. The Fourier maps (Fig. 2*a*) showed that the positional modulation of In and $P1O_4$ would better be described by a function that has one discontinuity within the x_4 interval. Therefore the saw-tooth function as introduced by Petříček *et al.* (1990) was applied (Figs. 2*b* and 2*c*); the result was a slight decrease of the *R* factors. Moreover a strong connection between In and $P1O_4$ allowed these atoms to be restricted. In the final calculation, four harmonic waves for the modulation of displacement parameters were used for K1, K2 and K3 and three for In. Crystal data and the main characteristics of the refinement are indicated in Table 1.

3.3. Results of refinement

The final coordinates, Fourier amplitudes of displacive modulation functions, equivalent isotropic displacement parameters for all atoms, and the anisotropic displacement parameters (ADP) and their modulated parameters are available in the supplementary material. The modulation parameters of the PO_4 rigid units are listed in Table 3.

3.3.1. Modulation of cations and cation–cation distances. The refined modulated structure answers the questions raised in the solution of the average structure. The disordered K4 cations are uniquely distributed over the intervals defined by the crenel functions. The atomic displacement parameters of all atoms are reasonable. The analysis of the cation–cation distance as a function of t confirms the validity of the suggested structure presentation (Figs. 1 and 3).

Both the saw-tooth modulated P1 atom and the three crenel positions of the P2 atoms maintain 12 P—P distances for every P atom (Fig. 4), and the P atoms (or more exactly PO_4 anions) subset exhibit a distorted hexagonal close packing. The large magnitudes of the P—P distances, which vary from 4.1 to 6.4 Å, arise from the shape of the PO_4 tetrahedral anion. The maximum 'diameter' of this rigid unit can be estimated as 5.8 Å = 2 × 2.9 Å [1.54 Å (P—O distance) + 1.36 Å (radius of O^{2-})], which confirms the higher limit of the variation.

As expected, the most prominent behaviour of the displacive parameters occurs for the K4 cation. This cation is continuously distributed within two t ranges (K4*a*, $\sim 0.1 < t < \sim 0.7$; K4*b*, $\sim -0.3 < t < 0.1$), which the cation switches between (Figs. 2 and 5). This behaviour is associated with the ordered distribution of K4 within the two P_4 tetrahedra that form the trigonal P_5 bipyramid (Fig. 3).

The modulations of all the other cations correlate with K4, as partially illustrated by the x_1–x_4 Fourier section (Fig. 2*a*). The principal tendency of the correlation is to maintain the second coordination sphere and coordination number (CN) of the In and K4 cations: $In[P,K]_{11}$ (distances 2.84–4.4 Å), $K4a[P,K]_{11}$ (distances 3.2–4.4 Å) and $K4b[P,K]_{10}$ (distances 3.15–4.5 Å), where K refers to the K1, K2 and K3 cations. The distances in the InP_5 trigonal bipyramid [one 2.84 (0.07) Å and four 3.1–3.7 Å,

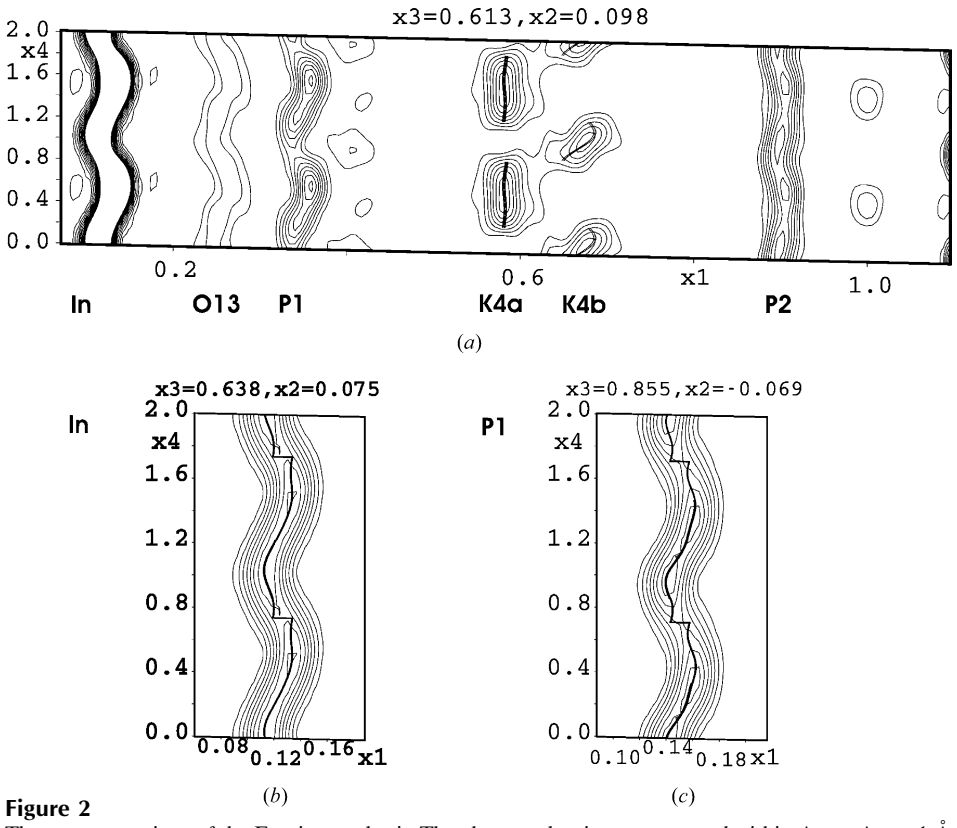

Figure 2
Three x_1–x_4 sections of the Fourier synthesis. The electron density was summed within $\Delta x_2 = \Delta x_3 = 1$ Å around the corresponding values indicated at the top. The crenel functions for K4*a* and K4*b* are shown in the centre of (*a*) ($0.1 < x_1 < 1.1$; $0 < x_4 < 2$; the contour step is 300 e Å^{-3}). The saw-tooth functions are shown in (*b*) for In (the contour step is 1000 e Å^{-3}) and in (*c*) for P1 (the contour step is 300 e Å^{-3}) atoms. The refined atomic modulation functions are indicated by bold lines.

Table 3
Modulation parameters of the PO_4 rigid units.

Wave	x_1 translation	x_2 translation	x_3 translation	φ rotation	χ rotation	ψ rotation
$P1O_4$ tetrahedron						
Saw-tooth function parameters: $x_4^0 = 0.242473\ (6)$; $\Delta x_1 = 0.0072$; $\Delta x_2 = 0.0079$; $\Delta x_3 = -0.0199$						
	0.00009 (5)	0.00055 (9)	0.00000 (7)	0.0	0.0	0.0
s,1	0.00342 (7)	−0.00331 (12)	0.00165 (10)	0.00275 (10)	−0.00384 (17)	0.00567 (15)
c,1	−0.00508 (6)	−0.01073 (11)	0.00055 (8)	0.00088 (9)	0.00590 (15)	−0.00789 (14)
s,2	−0.00116 (8)	−0.00461 (13)	−0.00413 (10)	0.00328 (11)	−0.00502 (19)	0.00143 (17)
c,2	−0.00157 (9)	0.00539 (13)	−0.00235 (12)	−0.00062 (12)	0.0032 (2)	−0.00019 (18)
s,3	0.00076 (18)	0.0054 (3)	0.0013 (2)	−0.0021 (2)	0.0039 (4)	0.0012 (4)
c,3	−0.00155 (17)	0.0027 (3)	−0.0021 (2)	0.0012 (2)	−0.0001 (4)	0.0002 (4)
$P2O_4$ tetrahedron						
Position *a*: $\Delta x_4 = 0.4132\ (13)$; $x_4^0 = 0.1130\ (8)$						
	0.00241 (8)	0.00651 (14)	0.00130 (11)	9.624	−0.587	−42.694
s,1	−0.0016 (10)	0.0037 (14)	−0.0002 (12)	−0.0012 (12)	0.007 (2)	0.0004 (19)
c,1	0.0013 (17)	−0.000 (2)	−0.000 (2)	−0.000 (2)	−0.003 (3)	0.000 (3)
Position *b*: $\Delta x_4 = 0.3799\ (13)$; $x_4^0 = 0.5051\ (10)$						
	−0.00228 (8)	−0.01017 (14)	−0.00190 (11)	−4.98 (18)	25.64 (15)	−42.60 (17)
s,1	−0.00316 (10)	−0.01626 (17)	0.00063 (13)	0.00031 (13)	0.0031 (2)	−0.0048 (2)
c,1	−0.00032 (16)	−0.00159 (23)	−0.00064 (21)	−0.0006 (2)	−0.0004 (4)	0.0000 (3)
Position *c*: $\Delta x_4 = 0.2070\ (13)$; $x_4^0 = 0.8025\ (14)$						
	−0.00018 (13)	0.00678 (21)	0.00116 (15)	−0.07 (19)	−0.37 (18)	−0.03 (17)

Fig. 5(*a*)] and in the $K4P_4$ tetrahedra [3.1–3.9 Å, Fig. 5(*c*)] are essentially shorter and more stable along the *t* coordinate than other distances in the corresponding polyhedra. In the InP_5 trigonal bipyramid, instead of six right angles there are three angles that vary around 100° and three angles that vary around 80° (Fig. 5*b*). This behaviour indicates a small shift of the In atom from the centre of the bipyramid into one tetrahedron.

The three crenel positions of the $P2O_4$ tetrahedron and its discontinuous rotation (Table 3) relate to the three kinds of K4 distribution within two edge-sharing $K4P_5$ trigonal bipyramids, as shown in Fig. 6. As seen from Fig. 6, whether the $P2O_4$ tetrahedron, which is located at the top of the trigonal bipyramid, is included in the $K4P_4$ (more specifically $K4[PO_4]_4$) tetrahedron depends on the kind of distribution.

The $K1P_6$, $K2P_6$ and $K3P_6$ octahedra are not regular and stable along the *t* coordinate (K—P distances vary from 3.3 to 4.4 Å). However, this second coordination sphere is more stable than the first sphere formed by O atoms. The number of O atoms varies between 6–7 for K1, 7–8 for K2 and 6–8 for K3 within the 2.4–3.2 Å range of the K—O distance.

3.3.2. Modulation of the PO_4 tetrahedra and InO_6 octahedron. In the three crenel ranges both the $P1O_4$ and the $P2O_4$

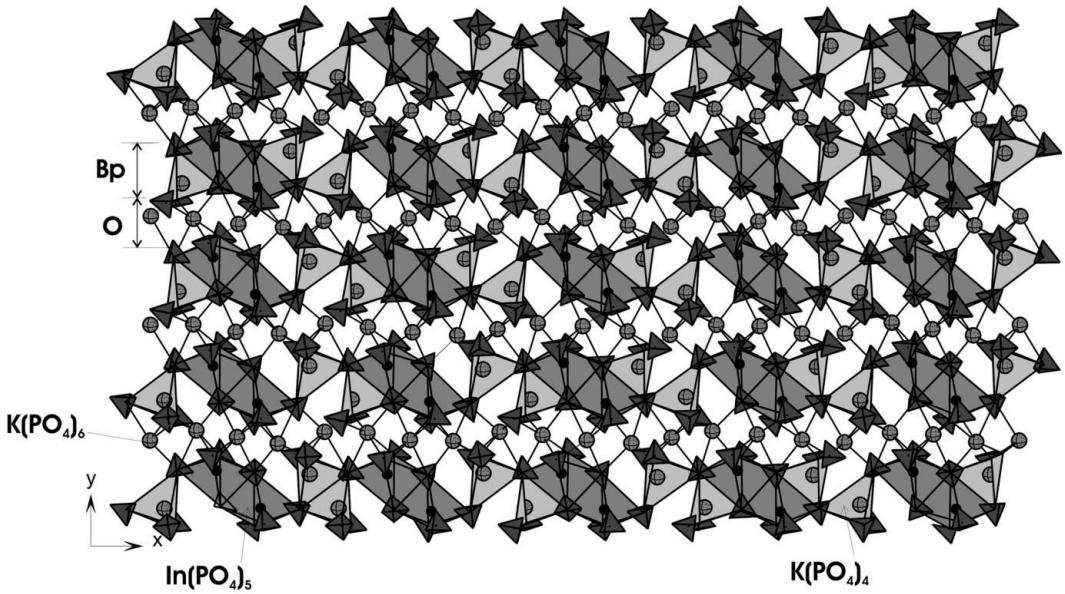

Figure 3
A portion of the characteristic layer normal to the [001] direction of the modulated structure. The *x* and the *y* axes correspond to the x_1 and x_2 directions, respectively. The Bp (bipyramid) and the O (octahedron) notations indicate the $P_5 = (PO_4)_5$ trigonal bipyramid portion and the $P_6 = (PO_4)_6$ octahedron portion, respectively. Every K4 cation is shifted into one tetrahedron (shown with light grey colour) within the $P_5 = (PO_4)_5$ bipyramid. The $K(PO_4)_6$ octahedra are indicated with six K—P sticks.

tetrahedra were refined as rigid units. Every tetrahedron has one non-shared O corner (O14 for P1 and O23 for P2) with a P—O distance (1.51 ± 0.01 Å) shorter than average (1.54 Å). The $P1O_4$ tetrahedron shares the O11—O12 edge with the InO_6 octahedron. The corresponding P1—O11 and P1—O12 distances [1.56 (0.01) Å] are slightly longer than the average value. The respective tetrahedron O11—P1—O12 angle is smaller [104 (1)°] while all other angles maintain the expected value [110 (2)°]. Within the more regular $P2O_4$ tetrahedron, the P—O distances and the tetrahedron angles vary less [1.54 (0.01) Å and 108 (1)°, respectively].

The In octahedron is formed with three O atoms (O11, O12, O13) that belong to the $P1O_4$ tetrahedron and three O atoms (O21, O22, O24) from $P2O_4$ (Fig. 7). The modelling of the modulation of the $P2O_4$ group by three crenel functions (labelled *a*, *b* and *c*) leads to four different combinations of groups adjacent to In: *aab*, *cca*, *bba* and *abc* (see Figs. 5–7), where the letters correspond to the crenel branches of the O21, O22 and O24 atoms, respectively. In the InP_5 trigonal bipyramid, the distances and angles (see Figs. 5*a* and 5*b*) are relatively stable over the full *t* range in spite of the existence of the four intervals. The discontinuous displacements of the P2 atoms at the borders cause a discontinuous rotation of the $P2O_4$ tetrahedron (Table 3) to complete the InO_6 octahedron (Fig. 7). Thus the stabilization of the InO_6 octahedron is the main reason of the $P2O_4$ tetrahedron rotation as a function of the *t* coordinates.

All of the InO_6 octahedra are distorted (Fig. 7). Their deformation results from the common O11—O12 edge, which is shared by the InO_6 octahedron and the $P1O_4$ tetrahedron. As in the tetrahedron the In—O11 and In—O12 distances [2.25 (0.10) Å] are longer than the other four [2.11 (0.12) Å]. The relatively short O11—O12 edge leads to a very small angle O11—In—O12 [(1) = 65.5 (0.9)° in Figs. 7(*b*) and 7(*c*)]. This angle does not vary essentially as a function of *t* (Fig. 7*b*). This stability is a consequence of the approximately constant P1—In distance (Fig. 5*a*) and relates to the constant shape of

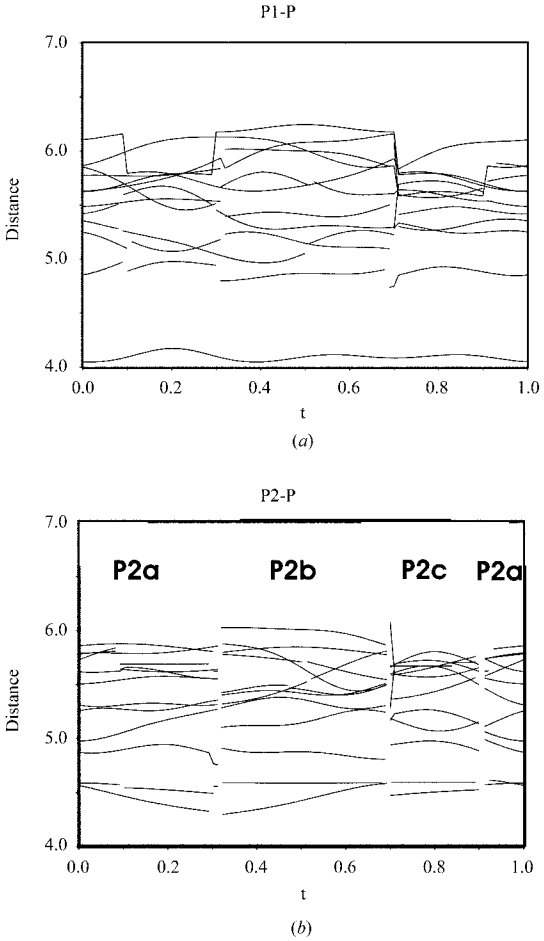

Figure 4
The P—P distances that characterize the close packing of the PO_4 tetrahedral anions in the modulated structure.

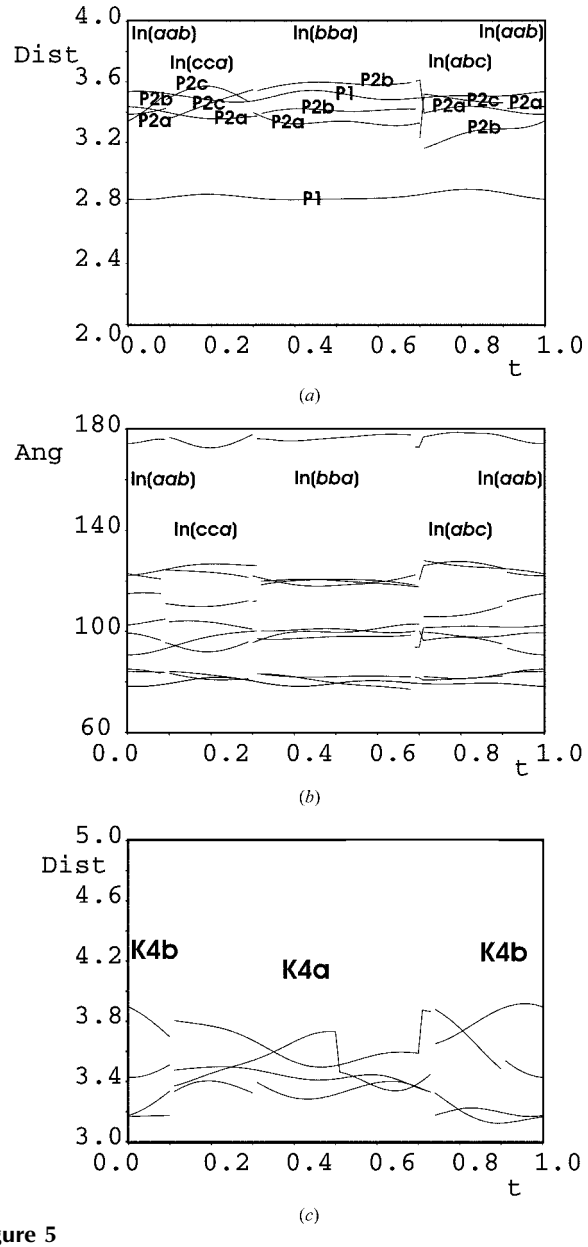

Figure 5
Geometrical characteristics of the In and K4 second coordination sphere as a function of *t* in the modulated structure: (*a*) distances and (*b*) angles in the InP_5 trigonal bipyramids; (*c*) distances in the $K4P_4$ tetrahedra.

the $P1O_4$ tetrahedron. The most relevant variations as a function of *t* relate to the angles (2), (3) and (4) (Figs. 7*b* and 7*c*). The distorted InO_6 octahedron tends to maintain the sum of the angles close to the ideal value of 360° (see Figs. 7*b* and 7*c*). In addition, the magnitude of a single angle can vary by up to 15% within a specific *t* range and up to 35% over the full range. The stabilization of the InO_6 geometry is the driving force of the $P2O_4$ rotation modulation. This can be accommodated by introducing a modulation of the O—In—O angle distortion.

4. Discussion

4.1. Origin of the $K_3In(PO_4)_2$ structure modulation

We assume that the main cause of the structure modulation is related to the ordering of the K4 cation over two P_4 (more specifically $[PO_4]_4$) tetrahedra that form the trigonal P_5 ($[PO_4]_5$) bipyramid within the hexagonal close packing of the PO_4 anions (Fig. 3). Three different kinds of the K4 environment within two P—P edge-sharing bipyramids lead to three positions of the P2 atom (Fig. 7*c*). Three P2 atoms and two P1 atoms form the InP_5 trigonal bipyramid, which is stable as a function of the *t* coordinate (Fig. 5*a* and 5*b*). Therefore, the modulation of P2 induces the modulation of the In and P1 atoms. The tendency to maintain the KP_6 octahedra, where K = K1, K2, K3, explains the modulation for the K1, K2 and K3 cations. The discontinuous rotation modulation of the $P2O_4$ tetrahedra allows the stabilization of the InO_6 octahedron.

4.2. Conformation of the origin of the $K_3In(PO_4)_2$ structure modulation

4.2.1. Chemical bonds in $K_3In(PO_4)_2$. The result of the modulated structure refinement allows us to trace the variability of the interatomic distances and draw a conclusion about the existence and stability of chemical bonds. Conversely, this analysis justifies the role of the structure modulation.

As expected, the P—O covalent bonds are the least variable and therefore the most stable entities in the framework. Therefore the PO_4 tetrahedral anions can be interpreted as building units similar to mono-atomic anions.

A comparison of the InP_5 bipyramid geometry (Figs. 5*a* and 5*b*) and the InO_6 octahedron geometry (Figs. 7*a* and 7*b*) shows that the magnitudes of both interatomic-distance and angle variations as functions of *t* are smaller for the second coordination sphere (the InP_5 bipyramid) than for the first (the InO_6 octahedron). Therefore, the In—P interactions are more stable than the In—O interactions in $K_3In(PO_4)_2$. Moreover, the shortest In—P distance [2.84 (0.05) Å], which is practically constant, is equal to the covalent In—P bond length (2.59–2.68 Å) that is found in the InP_4 tetrahedron (taking into account different CNs: 5 and 4, respectively). The InP_4 tetrahedron is a characteristic of the K_3InP_2 (Ohse *et al.*, 1993) and Na_3InP_2 (Blase *et al.*, 1991) alloys, which exhibit identical cationic composition and/or stoichiometry. Therefore the In—P interactions exist in the K_3InP_2 alloy and are partially conserved following the alloy's oxidation to $K_3InP_2O_8$ [= $K_3In(PO_4)_2$]. The presence of one covalent In—P bond in the $InP_5 = In[(PO_4)]_5$ trigonal bipyramid can explain the unusual common O—O edge shared by the $P1O_4$ tetrahedron and InO_6 bipyramid. The very short In—P distance (2.84 Å) does not permit a PO_4 tetrahedron and an InO_6 octahedron to share only a single O atom. On the other hand, it is clear that the five PO_4 tetrahedral anions that surround the In cation in the $In[(PO_4)]_5$ trigonal bipyramid can form six O corners of the InO_6 octahedron, where the PO_4 tetrahedra share at most two O atoms per tetrahedron (Fig. 7*c*).

Analogous arguments support the presence of K—P interactions in $K_3In(PO_4)_2$. In the K_3InP_2 alloy, the shortest K—P distances are equal to 3.25 and 3.28 Å. These values are close to the estimated covalent K—P bond (3.13 Å). In $K_3In(PO_4)_2$, the variation of the K—P distances in both KP_4 tetrahedra (K4*a*, 3.3–3.8 Å; K4*b*, 3.05–3.85 Å) and KP_6 octahedra (K1, 3.3–4.2 Å; K2 and K3, 3.3–4.6 Å) allows us to postulate the existence of K—P interactions, especially in the $K4P_4$ tetrahedra. A comparison of the first (oxygen) coordination sphere [the K4—O distances K4*a*, 2.65–3.3 Å (CN = 6–7); K4*b*, 2.4–3.3 Å (CN = 7–8)] and the second (phosphor) [CN = 4, the K4—P distances K4*a*, 3.3–3.8 Å; K4*b*, 3.15–3.9 Å (Fig. 5*c*)] shows that the second sphere is much more stable as a function of the *t* coordinate. The shift of the K4 cation from the centre of the $K4P_5$ trigonal bipyramids into $K4P_4$ tetrahedron can only be explained as a result of K—P interactions. The first (oxygen) coordination sphere varies essentially both in

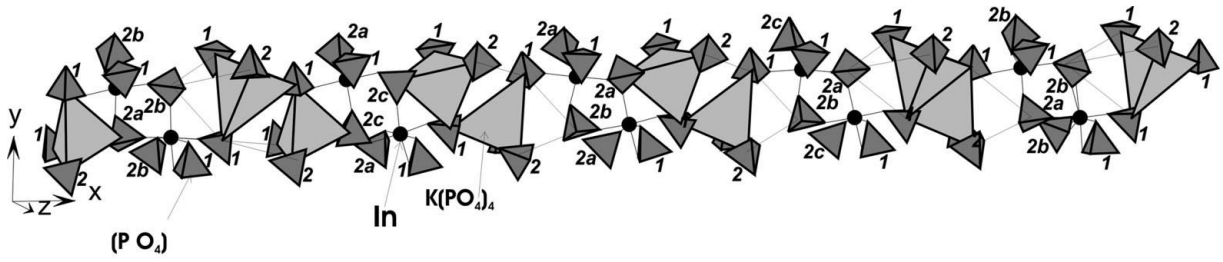

Figure 6
Portion of a chain of the $P_5 = (PO_4)_5$ trigonal bipyramids in the modulated structure. Light grey tetrahedra indicate the location of the K4 cations within the trigonal bipyramids. The $In(PO_4)_5$ bipyramids are represented by five PO_4 tetrahedral anions that surround every In cation (black circles). The notation 1, 2*a*, 2*b* and 2*c* refers to the corresponding PO_4 tetrahedra (Table 3). The six sticks connected to the black circles (In cations) and the corners of the tetrahedra (O atoms) indicate the InO_6 octahedron.

distances and in the CN with t for this atom, which confirms the K—P interaction in $K_3In(PO_4)_2$. Both In—P and K—P complex interactions must be considered as the driving forces for the modulations in this structure, where P plays the role of both an atom and the centre of the complex PO_4 anion.

4.2.2. Cationic array in α-, β-$Na_3In(PO_4)_2$, $Na_3Fe(PO_4)_2$, $Rb_3In(PO_4)_2$ and Na_3InP_2. The presence of the cation–[centre of anion] interactions in $K_3In(PO_4)_2$ justifies our proposed interpretation. Moreover, this description also seems to be valid and useful both for a large group of $A_{4-n}R_n(XO_4)_2$ compounds (A is an alkaline element; R = Y, Bi, In, rare earth or transition element; X = S, P, V, As; n = 0–4), which are related to the well known glaserite $[K_2Na(SO_4)_2]$ and/or the β-K_2SO_4 structure type, and for intermetallic compounds related to the Ni_2In structure type. The Ni_2In structure type is usually described as a hexagonal close packing of In atoms (anions); the Ni atoms (cations) are located in In_6 octahedra and In_5 trigonal bipyramids. Therefore, the formula can be expressed as $Ni^{[o]}Ni^{[bp]}In$. The cationic subset $A_{4-n}R_nX_2$ for the aforementioned oxides can be interpreted in the same way: X atoms (centres of complex anions) form the hexagonal close packing; A and R atoms (cations) fill the X_6 octahedra and X_5 trigonal bipyramids. The formula can be written as $(A,R)^{[o]}(A,R)^{[bp]}X$. In the oxides, which are similar to the Ni_2In-related compounds, the deformation and modification of the ideal structure is linked to the following factors: (i) the distribution and ordering of cations among octahedra and bipyramids; (ii) the distortion of the ideal close packing; (iii) the shifting of cations from the centre of the bipyramid toward the tetrahedron; (iv) the shifting of cations from the centre of octahedron. As can be seen, for example, from the work of Pearson (1972), in the Ni_2In-related compounds all these factors depend on both the relative size of the atoms and the covalent component of the bonds. Therefore, the same arguments can be applied for the oxides.

In order to lend support to the relative independence of the cationic subset and the role of the XO_4 entity, we compare four structures from the double phosphate family [α-, β-$Na_3In(PO_4)_2$E (Zhizhin *et al.*, 2000), $Na_3Fe(PO_4)_2$ (Morozov *et al.*, 2001) and $Rb_3In(PO_4)_2$ (Zhizhin *et al.*, 2002)] with the corresponding alloy Na_3InP_2 (Blase *et al.*, 1991) (Fig. 8, Table 4). As seen from Fig. 8, in comparison with Fig. 3, all these structures can be described by a distorted hexagonal close packing of P atoms (centre of PO_4 or P anions). Similarly

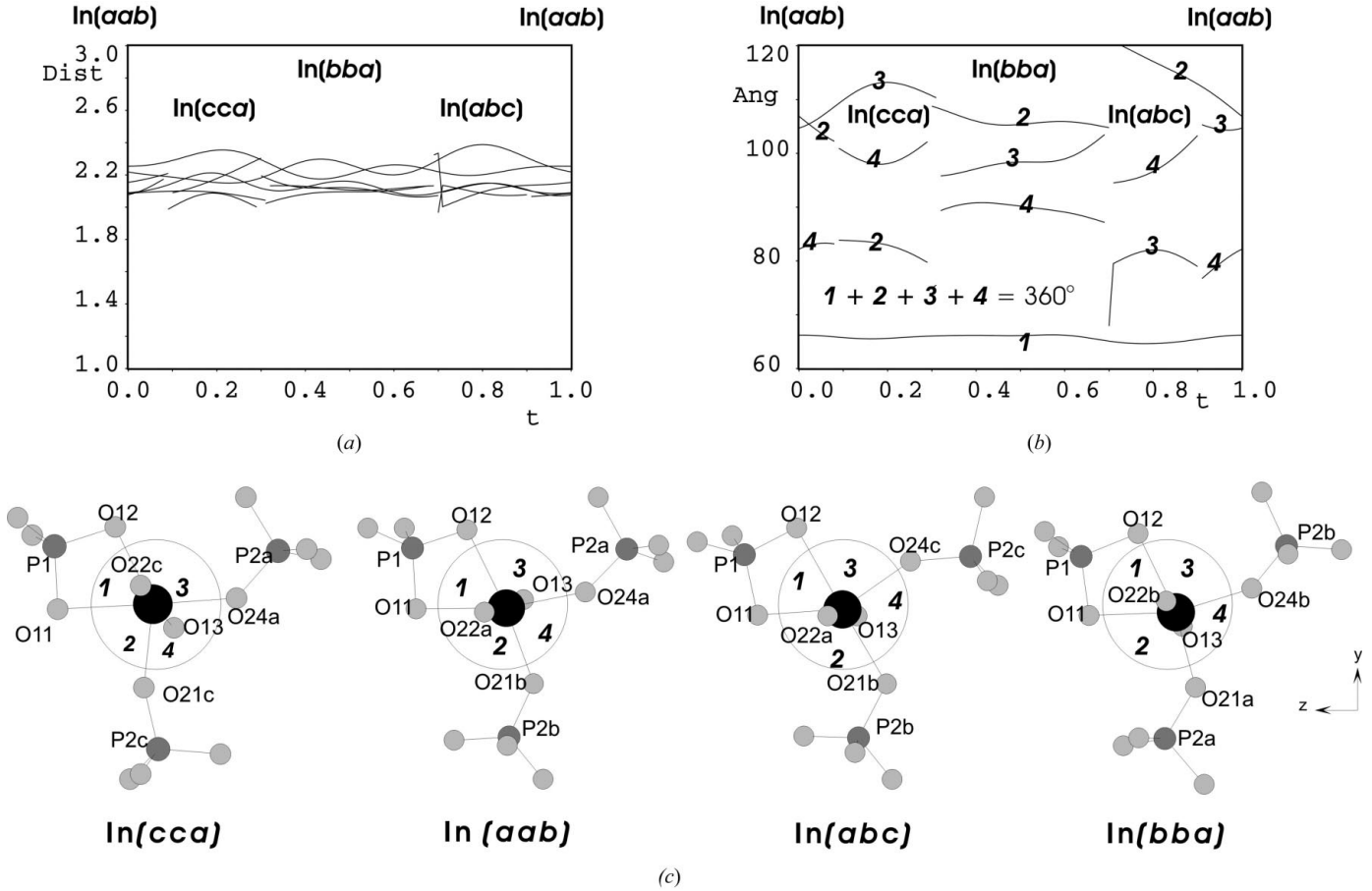

Figure 7
Geometrical characteristics of the first In coordination sphere and an illustration of their changes as a function of t in the modulated structure: (*a*) variation of the In—O distances and (*b*) the more flexible angles in the basis of the InO_6 octahedron within four t ranges (see the text for the labelling of the In surrounding); (*c*) illustration of different kinds of In surrounding in physical space. (1), the smallest acute angle O11—In—O12; (2) and (3), the supplementary angles O11—In—O21 and O12—In—O24, respectively; (4), opposite angle O21—In—O24. The labels *a*, *b*, *c* correspond to three crenel positions of the $P2O_4$ tetrahedron (Table 3).

Table 4
Distances (Å) in the cationic subset of $A_3RP_2O_8$ (A = Na, K, Rb; R = In, Fe) double phosphates compared with the Na_3InP_2 alloy.

	Na_3InP_2	α-$Na_3InP_2O_8$	β-$Na_3InP_2O_8$	$Na_3FeP_2O_8$	$K_3InP_2O_8$	$Rb_3InP_2O_8$
P—P						
Close packing; CN = 12	4.01–5.08 ⟨4.58⟩	4.08–5.54 ⟨4.51⟩	4.01–5.39 ⟨4.73⟩	4.14–5.19 ⟨4.85⟩	4.1–6.4 ⟨5.2⟩	4.05–6.44 ⟨5.27⟩
A—P						
Tetrahedron or bipyramid; CN = 4 (+ 1)	2.81–2.91 ⟨2.87⟩ (+ 4.47)	†3.00–3.49 ⟨3.16⟩ (+ 3.60)	†2.96–3.51 ⟨3.15⟩ (+ 3.81)	†2.84–3.40 ⟨3.09⟩ (+ 3.55)	†3.05–3.85 ⟨3.5⟩	†3.29–4.03 ⟨3.58⟩
Octahedron; CN = 6	2.86–4.12 ⟨3.31⟩	3.55–3.62 ⟨3.60⟩	3.41–3.79 ⟨3.57⟩	3.40–3.61 ⟨3.53⟩	3.3–4.4 ⟨3.75⟩	3.41–4.49 ⟨3.94⟩
R—P						
Tetrahedron or bipyramid; CN = 4 (+ 1)	2.59–2.68 ⟨2.635⟩	–	–	–	†2.84–3.5 (+ 3.6) ⟨3.36⟩	†2.82–3.56 (+ 3.59) ⟨3.37⟩
Octahedron; CN = 6	–	3.48–3.61 ⟨3.40⟩	3.40–3.48 ⟨3.43⟩	†3.28–3.42 ⟨3.35⟩	–	–

† The A—P and R—P bonds with the most likely covalent component.

to $K_3In(PO_4)_2$, the Na (Rb) and In (Fe) cations are distributed inside the octahedra and trigonal bipyramids. In each bipyramid, the cation is shifted into one of the two constituting tetrahedra. Different kinds of cationic distribution lead to the following:

(i) Different types of close-packing distortions. $Na_3Fe(PO_4)_2$ and $Na_3In(PO_4)_2$ exhibit octahedra that are more regular, in which 'strong' three-valence Fe^{3+} and In^{3+} cations are located. The Na and Rb octahedra in Na_3InP_2 and $Rb_3In(PO_4)_2$, respectively, are much more distorted and are similar to the K1, K2 and K3 octahedra in $K_3In(PO_4)_2$. Pairwise comparison of $Na_3Fe(PO_4)_2$/α-$Na_3In(PO_4)_2$ and $K_3In(PO_4)_2$/$Rb_3In(PO_4)_2$ shows the influence of the cation size inside the octahedron on the degree of close-packing distortion. In the close packing the P—P distances are independent of the presence of O atoms in the structure [compare $Na_3Fe(PO_4)_2$, $Na_3In(PO_4)_2$ and Na_3InP_2 in Table 4]. These distances depend only on the size of the cation located in the octahedra (compare K, Rb and Na compounds in Table 4).

(ii) Different types of the PO_4 disposition [compare the α and β modifications of $Na_3In(PO_4)_2$ in Fig. 8].

The role of the chemical bonds in the first coordination sphere of the In atom (six ionic covalent bonds In—O in the oxides and four covalent bonds In—P in the alloy) is revealed by the atom's different localization in the P_5 bipyramid. The In atom is practically undisplaced, *i.e.* at the centre of the bipyramid, in $K_3In(PO_4)_2$ and $Rb_3In(PO_4)_2$ [CN(In) = 5], whereas a maximal shift into the centre of the P_4 tetrahedron is observed in Na_3InP_2 [CN(In) = 4].

4.3. The modulated and the three-dimensional structure refinement of $K_3In(PO_4)_2$

The distinction between the previously determined three-dimensional structure (Zhizhin *et al.*, 2002) and the modulated refinement of $K_3In(PO_4)_2$ presented here must be raised. As seen in Table 2, all atomic parameters of the average structure of $K_3In(PO_4)_2$ are equivalent to the corresponding parameters reported for the three-dimensional structure refined from X-ray powder diffraction data. The slightly smaller displacement parameters can be related to the specific features of the Rietveld refinement technique; fixed atomic displacements and bond restraints have been used for the profile refinement procedure. The large temperature displacements of the K atoms and the much more important displacement of the O2n (n = 1–4) atoms compared with the O1n atoms are characteristic of both the average and the three-dimensional models. Moreover, the splitting in the K4 position was first revealed in the average structure of the modulated model and later used in the refinement of the three-dimensional model. This splitting resulted in an important decrease (from B_{iso} of ~7.5 to ~4 Å^2) of the K4 temperature displacement.

The absence of any satellite in the X-ray powder diffraction pattern was the only evidence for the existence of a three-dimensional phase. In order to compare the modulated structure solution obtained in the present work and the experimental powder X-ray diffraction data reported by Zhizhin *et al.* (2002), we used our incommensurate structure solution to calculate the corresponding diffraction profile . The modulated structure was refined from the same powder diffraction data with the program *JANA*2000 (Petříček & Dušek, 2000). All the structural parameters were fixed at values found from single-crystal data in order to keep the number of refined parameters within a reasonable limit. The characteristics of the refinement were slightly better than those for the three-dimensional structure model. Portions of the refined profiles are shown in Fig. 9. As can be seen, the experimental profile does exhibit very broad and weak background bulges at the highest satellite locations. The weaker satellites are practically non-visible in the calculated diagram.

Therefore, the X-ray powder diffraction experiment does not contradict the incommensurately modulated structure of the powder sample. On the other hand, this example does not allow us to detect an eventual modulated structure using X-ray powder diffraction data only.

5. Conclusions

The main conclusions of the present work are as follows.

The incommensurately modulated phase of $K_3In(PO_4)_2$ is the only phase that has been unequivocally identified at room temperature.

In the incommensurately modulated structure of $K_3In(PO_4)_2$:

(i) every PO_4 tetrahedral anion is a rigid building unit characterized by strong P—O covalent bonds and tetrahedral angles; the P—O bonds are much stronger than all other interatomic interactions including In—O;

(ii) the PO_4 anions form a hexagonal close packing; In cations fill half of the bipyramids; K cations are localized in all octahedra and in half of the bipyramids;

(iii) the origin of the structure modulation relates to the ordering of the K4 cations over the two tetrahedra that form the bipyramids; the modulation of all other cations follows the behaviour of K4, which conserves the K4–P interactions; the modulation of the O atoms follows the behaviour of the cations;

(iv) the translation modulations of the PO_4 tetrahedra are required in order to stabilize the cationic K_3InP_2 subset, while the rotation modulations of the $P2O_4$ tetrahedron are required for the InO_6 octahedron stabilization.

From the incommensurately modulated structures, the relative stability and power of chemical bonds can be deduced for certain compounds: the more stable an interatomic distance along *t*, the stronger the chemical bond.

Considerations of the cation–[centre of the anion] complex interaction can be used to describe and understand the stabilization of a large group of $A_3R(XO_4)_2$ compounds (*A* is

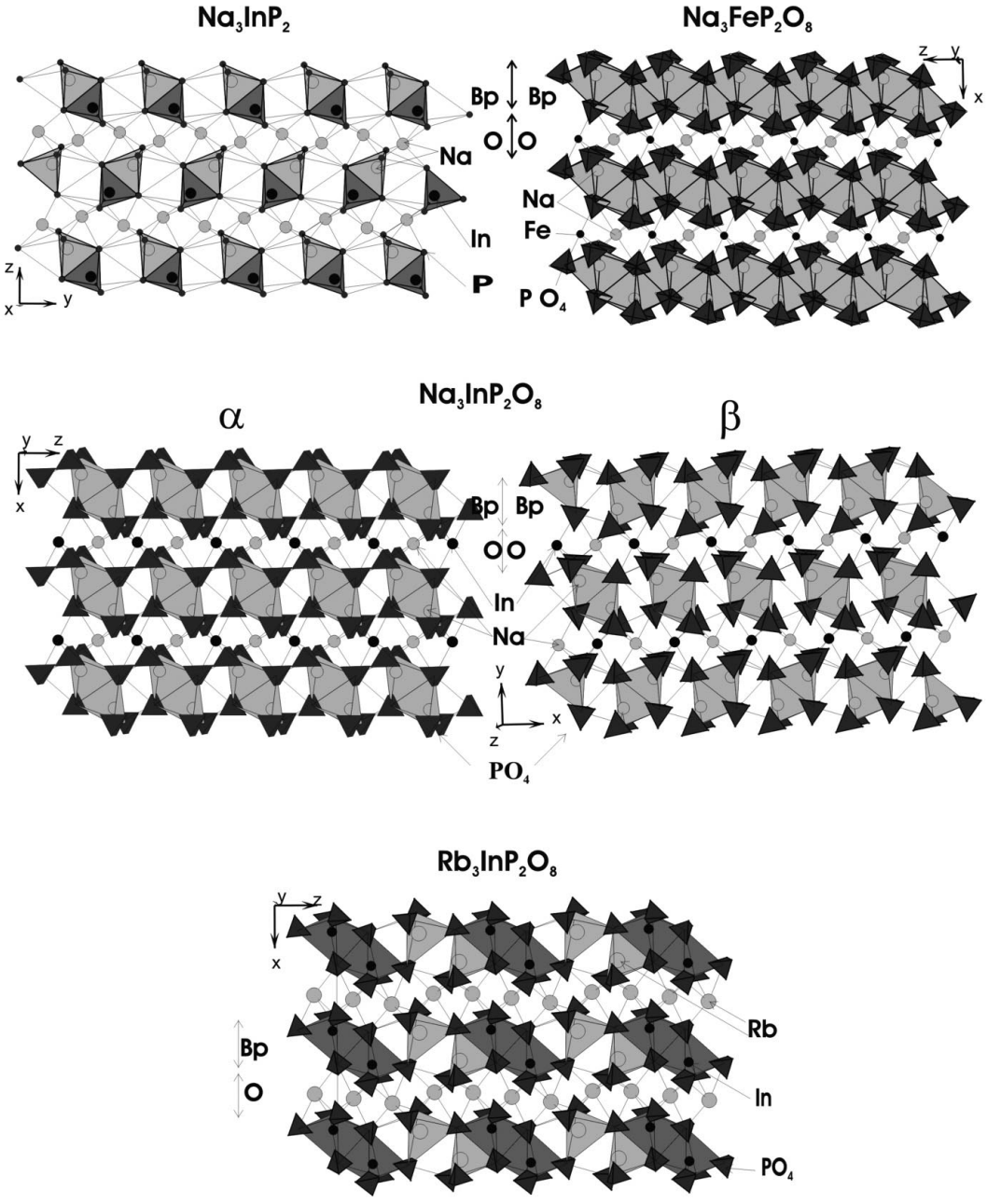

Figure 8
Comparison of $A_3R(PO_4)_2$ double phosphate structures (A = Na, Rb; R = Fe, In) and the Na_3InP_2 alloy. Characteristic layers similar to $K_3In(PO_4)_2$ are represented with a notation analogous to that in Fig. 3.

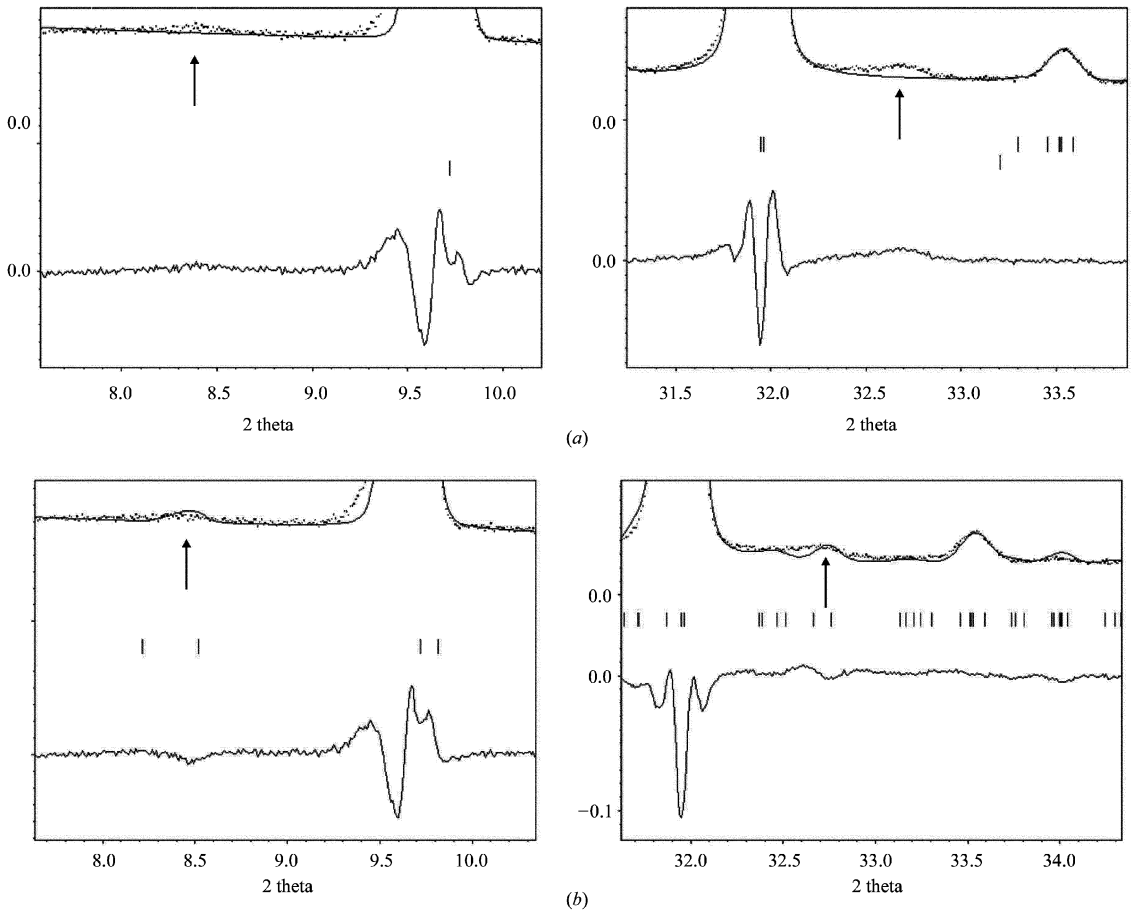

Figure 9
Two portions of the X-ray powder diffractogram approximated with (*a*) the three-dimensional structure refinement (Zhizhin *et al.*, 2002) and (*b*) the modulated structure refinement (present work). Dotted lines refer to the experimental data. In each case, the lower line is the residual; the arrows point to the location of satellite reflections.

an alkaline element; R = Y, Bi, In, rare earth or transferring element; X = S, P, V, As), all of them related to the well known glaserite [$K_2Na(SO_4)_2$] and/or the β-K_2SO_4 structure type.

The authors gratefully acknowledge Dr M. G. Zhizhin for supplying the crystals of $K_3In(PO_4)_2$ and for the X-ray powder diffraction data. We acknowledge the support of the Swiss National Science Foundation grant number 20–56870.99, the Herbette foundation of the University of Lausanne and the Grant Agency of the Czech Republic (grant 202/00/0645).

References

Blase, W., Cordier, G. & Somer, M. (1991). *Z. Kristallogr.* **195**, 119–120.
Morozov, V. A., Lazoryak, B. I., Malakho, A. P., Pokholok, K. V., Polyakov, S. N. & Terekhina, T. P. (2001). *J. Solid State Chem.* **160**, 377–381.
Ohse, L., Somer, M., Blase, W. & Cordier, G. (1993). *Z. Naturforsch. Teil B*, **48**, 1027–1034.
Oxford Diffraction Ltd (2001). *CrysAlis Software System.* Version 1.164 and 1.166. Oxford, England.
Pearson, W. B. (1972). *The Crystal Chemistry and Physics of Metals and Alloys.* New York/London/Sydney/Toronto: Wiley Interscience.
Petříček, V. & Dušek, M. (2000). *JANA*2000. *Structure Determination Software Programs.* Institute of Physics, Praha, Czech Republic.
Petříček, V., Gao, Y., Lee, P. & Coppens, P. (1990). *Phys. Rev. B*, **42**, 387–392.
Petříček, V., van der Lee, A. & Evain, M. (1995). *Acta Cryst.* A**51**, 529–535.
Schönleber, A., Meyer, M. & Chapuis, G. (2001). *J. Appl. Cryst.* **34**, 777–779.
Zhizhin, M. G., Filaretov, A. A., Olenev, A. V., Chernyshov, V. V., Spiridonov, A. V. & Komisarova, L. N. (2002). *Crystallogr. Rep.* **47**, 773–782.
Zhizhin, M. G., Morozov, V. A., Bobylev, A. P., Popov, A. M., Spiridonov, F. M., Komissarova, L. N. & Lazoryak, B. I. (2000). *J. Solid State Chem.* **149**, 99–106.